

Experimental and Numerical Investigation on the Irregularity of Carbonation Depth of Concrete Under Supercritical Condition

H. Bao, M. Yu, J. Ye, L. Xu and Y. Chi
Department of Civil Engineering, Wuhan University, China

J. Ye
Department of Engineering, Lancaster University, UK

ABSTRACT

The heterogeneity of a cement-based material results in a random spatial distribution of carbonation depth, which may significantly affect the mechanical properties and durability of the material. Currently, there is a lack of both experimental and numerical investigations aiming at a statistical understanding of this important phenomenon. This paper presents both experimental and numerical supercritical carbonation results of concrete blocks. The random fields of porosity and two-dimension random aggregate model of concrete were proposed for the simulation. The carbonation depths are measured and distributed along the carbonation boundary by the proposed rapid image processing technique, which are then statistically studied. The study has shown that considering the random distribution of coarse aggregates and using a random field of porosity with due consideration of spatial correlation and variance, the irregularity of carbonation depth can be realistically captured by the numerical model. Overall the methodology adopted in the paper can provide a foundation for future investigations on probability analysis of carbonation depth and other similar work based on multi-scale and -physics modelling.

Keywords: Carbonation depth, Concrete, Irregularity, Random aggregate model, Supercritical carbonation.

1.0 INTRODUCTION

Carbonation of cement based materials is a complex multi-physics process (Shen, Dangla, *et al.*, 2013; Maekawa, *et al.*, 2008; Zha, Yu, Ye, *et al.*, 2015; Phung, Maes, Jacques, *et al.*, 2016; Saetta, Schrefler, *et al.*, 1993), involving chemical reactions of CO₂ with CH and C-S-H; gas-liquid two phase flow; dispersion and diffusion of CO₂ in water and temperature propagation. Extensive research has been carried out on natural and accelerated carbonation, including the reviews on carbonation of cement-based materials (Aavija & Luković, 2016; Ashraf, 2016) and the life prediction model of cement-based materials under natural carbonation (Ann, Pack, Hwang, *et al.*, 2010; Enright, Frangopol, 1998). However, when the temperature and pressure exceed 304.12 K and 7.38 MPa, which are their respective critical values, CO₂ is in a supercritical fluid state that has a similar density of fluid and can diffuse through porous materials, such as cement based materials, like a gas (Rubin, Carey, Taylor, 1997). When the state of CO₂ is between supercritical fluid state and natural atmospheric environment, the carbonation of cement-based materials belongs to accelerated carbonation. Techniques have been developed in recent years to take advantages of the above carbonation processes to, e.g., modify composition and

microstructure of cement based materials (García-González, Hidalgo, *et al.*, 2006; Purnell, Seneviratne, Short, *et al.*, 2003; Feng, 2013) and to improve material properties using CO₂ curing (Zhan, Poon, Shi, 2013; Kou, Zhan, Poon, 2014). The techniques have also important applications in CO₂ capture and storage (Shen, Dangla, *et al.*, 2013), carbonation of hazardous water materials (Zha, Wang, Xie, *et al.*, 2016; Fernandezbertos, Simons, Hills, *et al.*, 2004; Venhuis & Reardon, 2001) and treatment of recycled concrete (Zhang, Shi, Li, *et al.*, 2015; Xuan, Zhan, Poon, 2016; Thiery, Dangla, Belin, *et al.*, 2013).

Carbonation depth is one of the most important characteristics that are used to define the extent of the chemical process taken place during carbonation. Experimental research has shown that under both natural (Beasley, 2015) and supercritical (Zha, Yu, Ye, *et al.*, 2015; Yu, Bao, Ye, *et al.*, 2017) conditions, the boundary topography of carbonation zones exhibits irregular shapes characterized by a random distribution of depth along the boundary with distinctive maximum and minimum. However, current theoretical and numerical models are almost exclusively based on the assumption that the materials are isotropic and homogenous (Samouh, Soive, Rozière, *et al.*, 2016), resulting in an uniform carbonation depth (Chang & Chen, 2006). There are very limited research on the irregularities of

carbonation depth, including (Huang, Jiang, Zhang, *et al.*, 2012) and (Huang, Jiang, Zhang, *et al.*, 2012)'s studies on the carbonation process of concrete where a non-uniform distribution of carbonation depth was observed by considering the influence of aggregates. It can be concluded that that it was the heterogeneity of cement-based materials that contributes mostly to the observed randomness (Ma, Zhang, Diao, 2015). This includes the presence of coarse aggregate (Yang & Cho, 2003), the carbon dioxide gas diffusion paths caused by distribution of cracks (Han, Liu, Wang, *et al.*, 2017) and the randomly distributed porosity of cement mortar (Yu, Bao, Ye, *et al.*, 2017). To study the irregularity of carbonation depth, (Huang, Jiang, Zhang, *et al.*, 2012) found that the variation of carbonation depth increased with increased use of coarse aggregates.

This paper attempts, as a pioneer work, to focus on investigating the irregularity of carbonation depth of concrete caused by randomly distributed porosity and coarse aggregates. Both supercritical carbonation experiments and multi-physics numerical simulations were carried out. The experimental investigation focus on the supercritical carbonation of concrete with different carbonation time. An image processing technique is proposed in this paper for the analysis of the experimental results. The numerical simulations are based on the multi-physics model (Zha, Yu, Ye, *et al.*, 2015), the random porosity of concrete (Yu, Bao, Ye, *et al.*, 2017) and the proposed two-dimension random aggregates model in this paper. The effects of autocorrelation lengths, coefficient of variation of porosity and coarse aggregate type on the irregularity of carbonation depth were discussed in this paper.

2.0 EXPERIMENTAL INVESTIGATION

2.1 Specimens Preparation

Concrete cubes with a dimension of 100 mm × 100 mm × 100 mm were cast for mercury intrusion porosimetry (MIP) to measure the average porosity of the material. The mix design proportions are given in Table 1. The specified 28-day cubic compressive strength of the cubes was 39 MPa. Ordinary Portland cement type P.O 42.5 was used as the binder for the mixtures. Normal river sands with fineness modulus of 2.7 were used as the fine aggregates.

Table 1. Mix proportions (kg/m³)

Constituent	Cement	Water	Sand	Gravel	water-binder ratio
Unit	kg/m ³	kg/m ³	kg/m ³	kg/m ³	-
OC	417.2	208.6	612.1	1162.1	0.5

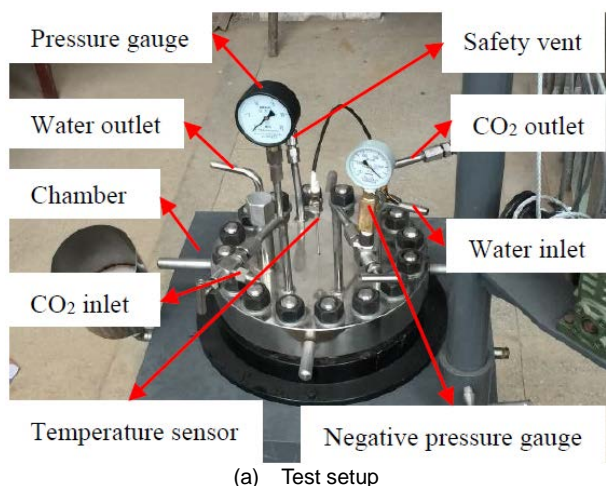
Nineteen concrete cubes were cast for the MIP and supercritical carbonation tests. After casting, the test specimens were covered with plastic sheets, and left in the casting room for 24 hrs. The specimens were then demolded and placed into a standard curing room with a constant temperature of 20 °C and humidity of 95% until the 28-day strength was achieved. Eighteen of the cured cubes were divided into 3 groups, each of which had six samples, for the supercritical carbonation test. The remaining one cube was used for the MIP. Three small cubic samples of approximately 1 cm³ were taken at different locations of the cement mortar cube mentioned above and tested by mercury intrusion porosimetry to obtain the average porosity of the cement mortar cube. Then the samples were immersed in absolute ethyl alcohol to avoid further hydration. The threshold pressure was 7.11 MPa for MIP. The average porosity, measured by MIP, is 12.8% and then used in the following Sections as the average porosity of the concrete before carbonation.

2.2 Tests Procedure and Setup

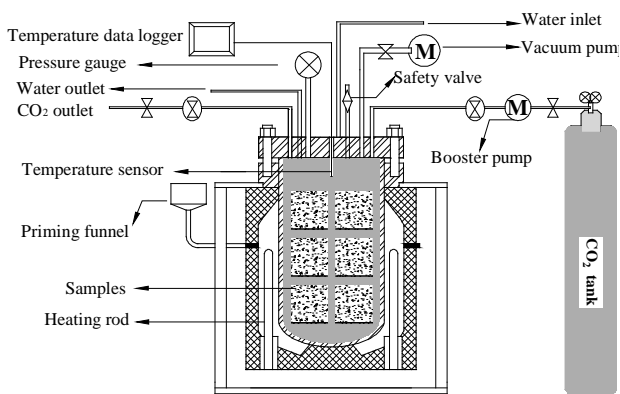
The supercritical carbonation tests were performed using a closed-cycle carbonation system that included a sealed chamber, a vacuum pump, an air compressor, a booster pump and a CO₂ cylinder unit, as shown in Fig 1. Fig. 1 also shows that a temperature data logger, a pressure gauge and heating rods were mounted to the sealed chamber. For a typical test, 6 cubes can be placed in the chamber.

Before CO₂ gas injection, the chamber was vacuumed to -0.98 bar by the vacuum pump. CO₂ gas was injected to the chamber driven by the pressure gradient between the CO₂ tank and the chamber. The CO₂ pressure and temperature in the chamber were controlled by a gas regulator. When the pressure in the CO₂ tank was reduced and close to that of the chamber, the air compressor started to run to maintain the injection flow until the desired pressure and temperature in the chamber were achieved and kept at a constant level.

The three groups of cubes were then subjected to three different carbonation time periods with the temperature and atmospheric pressure exceeding, respectively, 304.12 K and 7.38 MPa. The pressure and temperature in the chamber were constantly monitored and recorded. The respective recorded temperature and pressure for a total carbonation time of 4.7 h, 5.3 h and 7.5 h, in which the respective supercritical carbonation time were 3 h, 4 h and 5 h. The total carbonation time includes the inflating time, the supercritical carbonation time and the CO₂ recycling time, denoted, respectively, by the ascending, plateaued and descending branches. Fig. 2 shows the recorded temperature and pressure for a total carbonation time of 7.5 h, in



(a) Test setup



(b) Details of reaction still

Fig. 1. Details of closed-cycle carbonation system for concrete

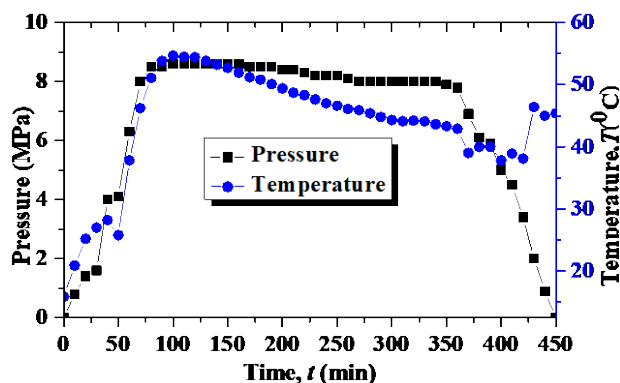
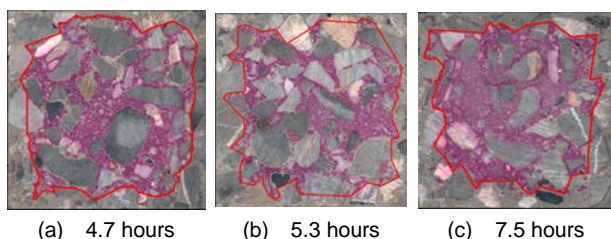


Fig. 2. Conditions of supercritical carbonation



(a) 4.7 hours (b) 5.3 hours (c) 7.5 hours

Fig. 3. Test results of supercritical concrete carbonation

which the supercritical carbonation time is 5 h. During the tests, the surrounding relative humidity was also recorded.

After the supercritical carbonation process was completed, the CO₂ gas was recycled to the CO₂ tank. The carbonated concrete cubes were removed from the chamber.

3.0 EXPERIMENTAL RESULTS AND IMAGE PROCESSING

3.1 Test Results of Supercritical Carbonation

The carbonated concrete cubes removed from the chamber were cut into two halves. The fresh cuts of the cubes were polished and cleaned. Phenolphthalein solution was sprayed on the cuts to reveal any non-carbonated zones identified by pink color, which also revealed the boundaries separating the carbonated and non-carbonated zones on the cuts. The colored surfaces were then scanned by a scanner. The scanned images are shown in Figs. 3 (a), (b) and (c), showing the cuts from the cubes carbonated for 4.7 h, 5.3 h and 7.5 h, respectively.

As shown in Fig. 3, the non-carbonized zones are all around the centers of the blocks and all have irregular boundaries of random nature. As a result, the maximum and minimum carbonation depths on a cut are significantly different, and are also of random nature.

3.2 Imaging Processing of the Irregular Carbonation Depth

Fig. 4(a) shows the carbonation boundary of the concrete carbonation profile in Fig. 3(a), which was from the scan image processed by Matlab as an assembly of pixels. To plot the carbonation depth against the location along the boundary in a rectangular co-ordinate system, the four corner points, identified as A, B, C and D at the carbonation boundary are first located. The four points have the shortest distances to their respective nearest vertices formed by the edges of the section, as shown in Fig. 4(a). Starting from point A, the distances from the carbonation boundary to the edge of the cube were measured and are presented as the carbonation depth in Fig. 4(b).

The above procedure was applied to all the samples to record the distribution of the carbonation depth of all the tested concrete blocks, carbonated, respectively, for 4.7, 5.3 and 7.5 hours. In summary, the carbonation depths of all of them, carbonated for 7.5 hours, starting from point A are shown in Fig. 5, where the average carbonation depths of each samples are also shown. The carbonation depths are randomly distributed for all the cases.

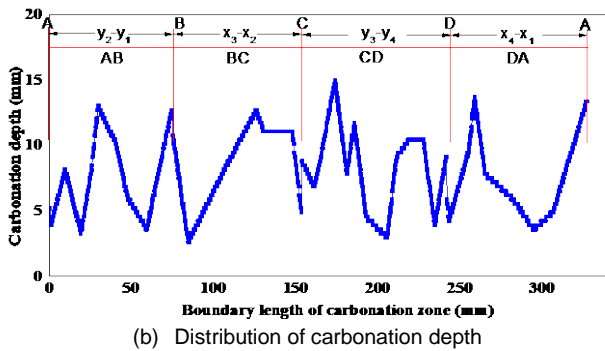
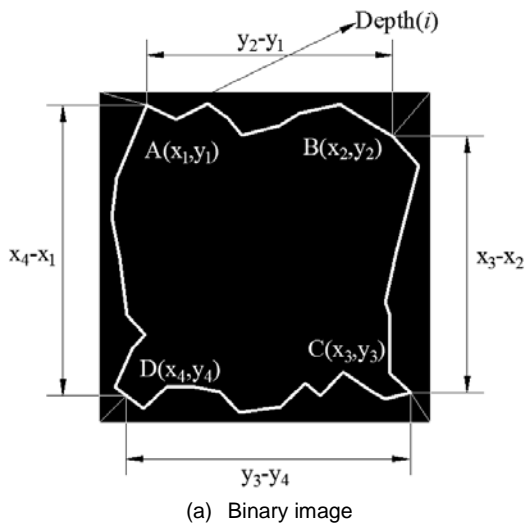


Fig. 4. Distribution of the measured carbonation depth

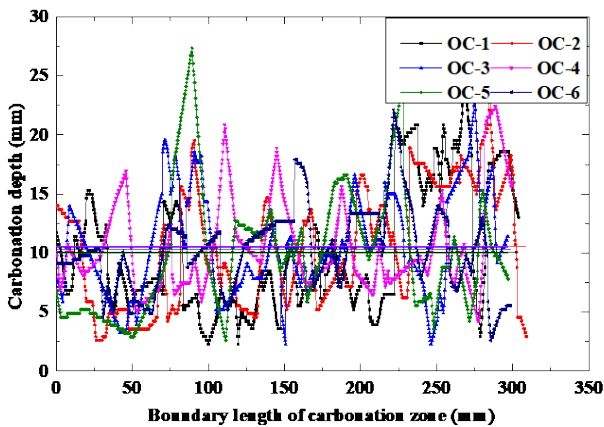


Fig. 5. The distribution of carbonation depth around the boundary length of carbonation zone of test results

3.3 Average and Variance of the Irregular Experimental Carbonation Depth

In this section, the randomly distributed carbonation depths of the tested blocks were characterized by their average, maximum and minimum carbonation depths, which were extracted from Fig. 5 and presented in Fig. 6. It can be seen that within a group of the concrete blocks, the average

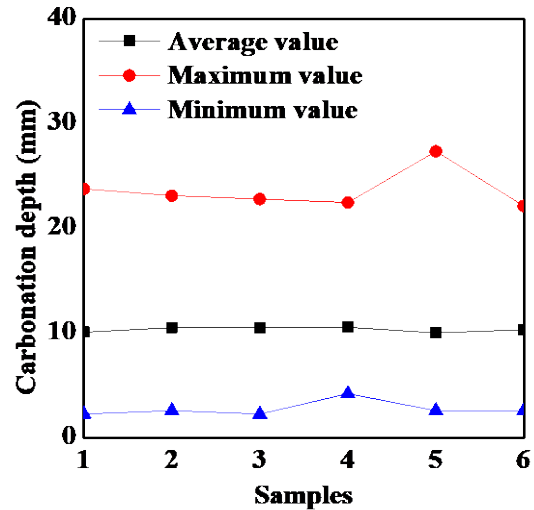


Fig. 6. Test results of carbonation depth of concrete samples

carbonation depths across the 6 samples agree with each other reasonably well, while the maximum and minimum carbonation depths across the six samples exhibit greater discrepancies.

Table 2 presents the average carbonation depths and their variances across the six samples of each groups. As expected, the results show that both the average and the variance of the carbonation depths from the experiments increase with the increase of carbonation time.

Table 2. Average values of average carbonation depth and their variances of test blocks

Group	Carbonation time, T (h)	Average value	
		Average carbonation depth, μ_1 (mm)	Variance, v_1 (mm ²)
Group 1	4.7	8.3	10.7
Group 2	5.3	8.6	14.8
Group 3	7.5	10.3	21.0

4.0 NUMERICAL INVESTIGATION

The irregularity of carbonation depth of concrete can be found in all the test cubes. Therefore, the average value and variance of test carbonation depths of concrete were statistically analyzed in Section 3. The irregularity of carbonation depth of concrete was influenced by the randomly distributed aggregates and porosity. In order to study the effect of the above two factors on the irregularity of carbonation depth. The random aggregates model and random fields of porosity model were adopted in this section. The effects of autocorrelation length, coefficient of variation of porosity and coarse aggregate type on the irregularity of carbonation depth were mainly studied. In this section, the simulation results of the test cases were summarized and compared with the experimental results presented in Section 3.

4.1 Introduction of the Numerical Simulation Method of Irregularity of Carbonation Depth

In order to simulate the process of supercritical carbonation, the random aggregate model for concrete was proposed. This model provides with a method to generate the two-dimension random aggregate for concrete rapidly. The generative process of random aggregate model for concrete are shown in Fig. 7.

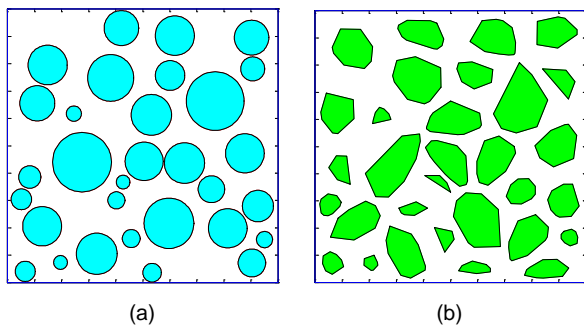


Fig. 7. The generative process of random aggregate model for concrete (0.10 m×0.10 m)

The mix proportion and aggregate gradation of concrete in the following example can be set. For illustration, the information of the quality of cement, sand, stone, water and the aggregate gradation derived from Section 2.1. The technical proposal can be concluded as follows.

The two-dimensional random circular aggregates model was generated by means of Monte Carlo method according to the given mix proportion, aggregate gradation and sectional dimension of concrete. Then the coordinates of centre point and area of each circular aggregate were obtained, as shown in Fig. 7(a). The area of each convex polygon, with the same centre point coordinate of circular aggregate in Fig. 7(a), was shrank to make sure that the area was equal to the area of circular aggregate. The shrunken convex polygons form the two-dimension random gravel aggregate model, as shown in Fig. 7(b).

The method to generate the two-dimension random aggregate model of concrete possesses simple operating steps, reasonable design, better performance and lower cost. The generation of random aggregates needs less computational cost that the method can be applied in numerical simulation.

In this section, the test results presented in Section 3 were used to validate the average carbonation depth and the variance of the carbonation depth predicted by the 2-D Multiphysics supercritical carbonation model developed previously by the authors (Yu, Bao, Ye, *et al.*, 2017), where a random field of porosity of cement based on the method of the modified ellipsoidal autocorrelation function was

used to simulate the random voids distribution. The developed random field model of porosity offered a porosity distribution ranged from 0 to 1 and considered spatial correlation by selecting the values of a and b , and is as follows (Yu, Bao, Ye, *et al.*, 2017).

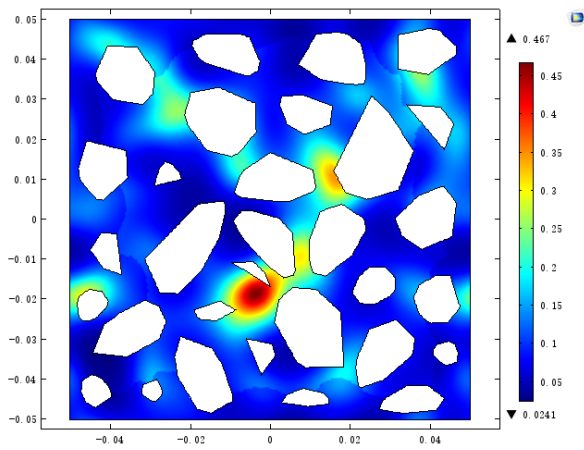
$$\phi(x, y) = \exp \left[-\left(\frac{x^2}{a^2} + \frac{y^2}{b^2} \right)^{\frac{1}{1+r}} \right] \quad (1)$$

where ϕ is an ellipsoidal autocorrelation function; a and b are the autocorrelation lengths in the x and y directions, respectively; r is the roughness factor (when $r=0$, it is the Gaussian autocorrelation function). In the previous work, it was assumed that the autocorrelation lengths, a and b , in equation (1) were both 0.005 m (Yu, Bao, Ye, *et al.*, 2017). It was observed that the introduction of spatial correlation resulted in more realistic results than those from other random models without considering it. The random porosity model of concrete blocks, considering the spatial correlation, can satisfactorily capture the irregular boundaries of the non-carbonated zones. Therefore, it is clear that the autocorrelation lengths, a and b , and coefficient of variation of porosity, CV_p , have played import roles in defining the topography of the carbonation front. To simulate the random nature of the carbonation front, there are three main parameters that have to be considered, including the average porosity, the autocorrelation lengths and the coefficient of variation of porosity. The average porosity, 0.12 in this case, can be obtained by mercury intrusion porosimetry.

4.2 Effects of Autocorrelation Lengths and Coefficient of Variation of Porosity on the Irregularity of Carbonation Depth

The above mentioned two-dimension random aggregate model of concrete, according to the mix proportion and aggregate gradation in Section 2.1, was applied in this section. In order to numerical study the effects of the autocorrelation lengths and the coefficient of variation of porosity on the carbonation depth of concrete. A representative distribution of initial porosity, derived from the MIP in Section 2.1 and $a=b=0.01$ m, $CV_p=0.5$, with a representative aggregate distribution of the random aggregate model of concrete was shown in Fig. 8.

All the concrete blocks tested in Section 3 were simulated in the supercritical condition using the numerical model presented in (Zha, Yu, Ye, *et al.*, 2015) with a total carbonation time of 4.7, 5.3, 7.5 hours, respectively. For a given carbonation time, 6 samples with the same coefficient of variation and autocorrelation length were studied. For given values of a , b and CV_p , 18 samples with varying properties were simulated. Therefore, a total of 162 cases were studied.



considering the random distribution of porosity (m)

In order to study the effects of the above two factors on the topography of carbonation depth, random porosity with autocorrelation lengths of $a=b=0.005$ m, 0.008 m, 0.01 m and coefficient of variation of porosity $CV_p=0.1, 0.3, 0.5$ were studied. The average initial porosity is 0.12 from the mercury intrusion porosimetry test in Section 2.1.

The random porosity field with different autocorrelation lengths, coefficients of variation of porosity and fixed carbonation time $T=7.5$ hours are shown in Fig 9.

Fig. 8. The random aggregate model of concrete

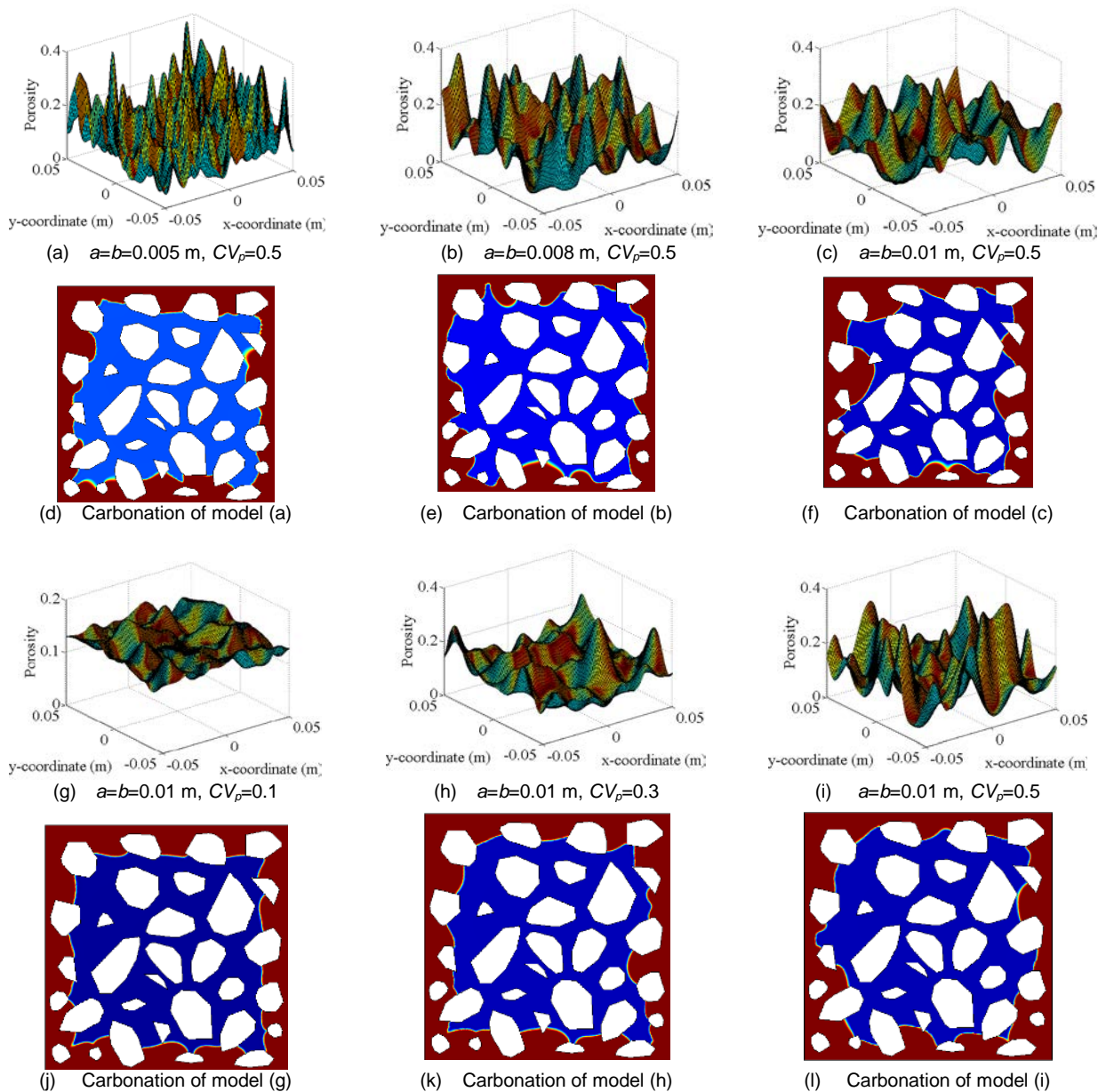


Fig. 9. Random distribution of porosity and the corresponding carbonation results

Figures 9 (a), (b) and (c) show the porosity distribution of a concrete that has a fixed coefficient

of variation of porosity $CV_p = 0.5$ and varying autocorrelation lengths, i.e., $a=b=0.005$ m, 0.008 m,

0.01 m. Their respective carbonation profiles are shown in Figs. 9 (d), (e) and (f), where the effect of spatial correlation on carbonation depth is evident. Figs. 9 (g), (h) and (i) are the porosity distribution of the concrete with varying coefficient of variation of porosity $CV_p = 0.1, 0.3$ and 0.5 , while the autocorrelation length was fixed to $a=b=0.01$ m. The respective carbonation results are shown in Figs. 9 (j), (k) and (l).

Table 3. Average values of average carbonation depth and variance

Carbonation time, T (h)	Autocorrelation length, $a=b$ (m)	Coefficient of variation of porosity, CV_p	Average value	
			Carbonation depth, μ_1 (mm)	Variance, v_1 (mm ²)
7.5	0.005	0.1	10.7	1.6
7.5	0.005	0.3	11.0	5.1
7.5	0.005	0.5	10.9	8.4
7.5	0.008	0.1	11.0	1.8
7.5	0.008	0.3	10.6	8.5
7.5	0.008	0.5	10.3	13.1
7.5	0.01	0.1	10.9	1.9
7.5	0.01	0.3	11.2	7.4
7.5	0.01	0.5	10.7	17.8

From the simulation results, the average carbonation depths and their average values of variance of each of the groups were calculated and listed in Table 3. As expected, the effect of the autocorrelation lengths on the average carbonation depth are not significant. The variance of carbonation depth increases with an increase of the autocorrelation lengths, which explains well why use of the modified ellipsoidal autocorrelation function can pick up the random nature of carbonation depth caused by random porosity. The variance of carbonation depth increases also with an increase of the coefficient of variation of porosity. The effect of the coefficient of variation of porosity on the average carbonation depth are not significant.

4.3 Effects of Coarse Aggregate Type on the Irregularity of Carbonation Depth

In order to study the effects of coarse aggregate type with random porosity distribution on the irregularity of carbonation depth. The variation of temperature and pressure derive from the test results as shown in Fig. 2. The total carbonation time is 7.5 h. The mix proportion and coarse aggregate gradation derive from Section 2.1. The coarse aggregate type were circular aggregates and crushed stone aggregates. The specific parameters were shown in Table 4.

The parameters in Table 4 were employed to generate the random porosity fields and two-dimensional random aggregate model. The random distribution of porosity is shown in Fig. 10(a).

Moreover, in order to eliminate the effects of random number on carbonation results. Six random aggregate model with the same coarse aggregate gradation and same porosity distribution were applied to simulate the supercritical carbonation.

Table 4. Parameters for the supercritical carbonation of concrete of different coarse aggregate type with random porosity distribution

Coarse aggregate type	Circular aggregate	Crushed stone aggregate
Average porosity, ϵ_m		0.122
Initial intrinsic permeability coefficient, k_0 (m ²)		3×10^{-21}
Autocorrelation length, $a=b$ (m)		0.01
Coefficient of variation of porosity, CV_p		0.5
Supercritical carbonation time, T_c (h)		5

Only one of the six carbonation results of different coarse aggregate type was presented as shown in Figs. 10(b-c). The distribution of carbonation depth of the model in Fig. 10 were obtained. By statistically analyzing the distribution of carbonation depth. The average value of average, maximum and minimum carbonation depth and variance of carbonation depth of the six model were list in Table 5. As shown in Table 5, it is a numerical nature that the value of average, maximum, minimum and variance of carbonation depth of crushed stone aggregates are very close to that of circular aggregates under the same conditions. The effect of aggregates type on the supercritical carbonation of concrete is not obvious.

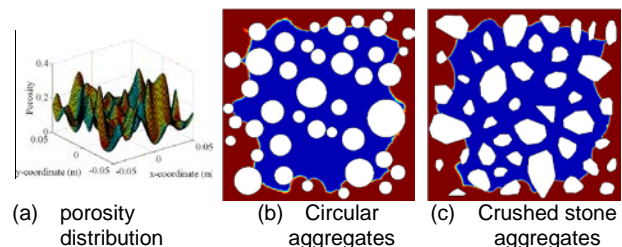


Fig. 10. The carbonation results of concrete of different coarse aggregate type with random porosity distribution

Table 5. Average values of average, maximum and minimum carbonation depth and their variances of different coarse aggregate type with random porosity distribution

Coarse aggregate type	Circular aggregate	Crushed stone aggregate
Average carbonation depth, D (mm)	10.9	10.9
Maximum carbonation depth, D_{max} (mm)	19.5	19.5
Minimum carbonation depth, D_{min} (mm)	4.4	4.5
Variance, v_2 (mm ²)	12.5	11.8

5.0 CONCLUSIONS

Experimental and numerical investigations on the irregularity of supercritical carbonation depth of concrete have been presented in this paper. The irregularity of supercritical carbonation depth of concrete was modelled by introducing random field of porosity and two-dimension random aggregate model to simulate the heterogeneous geometry of the carbonation profile. An image processing technique was proposed to effectively capture the distributions of carbonation depth from both the experiments and simulations. The random nature of the carbonation depths was then studied statistically by calculating the relevant average, variance. From the present study, the following conclusions can be drawn:

- a) The proposed image processing technique can be used satisfactorily to capture the random distribution of carbonation depth of concrete.
- b) The variance of the numerical irregular carbonation depth increase with the increase of coefficient of variation of porosity.
- c) It is a numerical nature that effects of aggregates type on the value of average, maximum, minimum and variance of carbonation depth are not obvious.

Acknowledgement

The authors are grateful for the financial support from the National Key Research and Development Program of China (2016YFC0701400).

References

- Aavija, B., Luković, M., 2016. Carbonation of Cement Paste: Understanding, Challenges, and Opportunities. *Construction and Building Materials*, 117:285-301.
- Ann, K.Y., Pack, S.W., Hwang, J.P., Song, H.W., Kim, S.H., 2010. Service Life Prediction of a Concrete Bridge Structure Subjected to Carbonation. *Construction and Building Materials*, 24(8):1494-1501.
- Ashraf, W., 2016. Carbonation of Cement-Based Materials: Challenges and Opportunities. *Construction and Building Materials*, 120:558-570.
- Beasley, K.J., 2015. Carbon Dating Concrete Cracks. *Journal of Performance of Constructed Facilities*, 29(025140021).
- Chang, C., Chen, J., 2006. The Experimental Investigation of Concrete Carbonation Depth. *Cement and Concrete Research*, 36(9):1760-1767.
- Enright, M.P., Frangopol, D.M., 1998. Service-Life Prediction of Deteriorating Concrete Bridges. *Journal of Structural Engineering*, 124(3):309-317.
- Feng, G., 2013. Experimental and Numerical Study of Accelerated Carbonation in Cement Brick and Tile. Harbin Institute of Technology, Master Degree in Engineering. (in Chinese)
- Fernandezbertos, M., Simons, S., Hills, C., Carey, P., 2004. A Review of Accelerated Carbonation Technology in the Treatment of Cement-Based Materials and Sequestration of CO₂. *Journal of Hazardous Materials*, 112(3):193-205.
- García-González, C.A., Hidalgo, A., Andrade, C., Alonso, M., Fraile, J., 2006. Modification of Composition and Microstructure of Portland Cement Pastes as a Result of Natural and Supercritical Carbonation Procedures. *Industrial & Engineering Chemistry Research*, 45(14):4985-4992.
- Han, J., Liu, W., Wang, S., Geert, D.S., 2017. Carbonation Reaction and Microstructural Changes of Metro-Tunnel Segment Concrete Coupled with Static and Fatigue Load. *Journal of Materials in Civil Engineering*, 29(040162162).
- Huang, Q., Jiang, Z., Zhang, W., Gu, X., Dou, X., 2012. Numerical Analysis of the Effect of Coarse Aggregate Distribution on Concrete Carbonation. *Construction and Building Materials*, 37:27-35.
- Kou, S., Zhan, B., Poon, C., 2014. Use of a CO₂ Curing Step to Improve the Properties of Concrete Prepared with Recycled Aggregates. *Cement and Concrete Composites*, 45:22-28.
- Maekawa, K., T.I., T.K., 2008. Multi-Scale Modeling of Structural Concrete, Taylor&Francis.
- Ma, R., Zhang, J., Diao, B., 2015. Research on the Carbonation Model of Stress Concrete Components. *Advances in Intelligent Systems Research*, 191-195.
- Phung, Q.T., Maes, N., Jacques, D., De, Schutter, G., Ye, G., 2016. Modelling the Carbonation of Cement Pastes under a CO₂ Pressure Gradient Considering both Diffusive and Convective Transport. *Construction and Building Materials*, 114:333-351.
- Purnell, P., Seneviratne, A.M.G., Short, N.R., Page, C.L., 2003. Super-Critical Carbonation of Glass-Fibre Reinforced Cement. Part 2: Microstructural Observations. *Composites Part a: Applied Science and Manufacturing*, 34(11): 1105-1112.
- Ruan, X., Pan, Z., 2012. Mesoscopic Simulation Method of Concrete Carbonation Process. *Structure and Infrastructure Engineering*, 8(2):99-110.
- Rubin, J.B., Carey, J.W., Taylor, C., 1997. Enhancement of Cemented Waste Forms by Supercritical CO₂ Carbonation of Standard Portland Cements, 473-478.
- Saetta, A.V., Schrefler, B.A., Vitaliani, R.V., 1993. The Carbonation of Concrete and the Mechanism of Moisture, Heat and Carbon-Dioxide Flow-through Porous Materials. *Cement and Concrete Research*, 23(4):761-772.

- Samouh, H., Soive, A., Rozière, E., Loukili, A., 2016. Experimental and Numerical Study of Size Effect on Long-Term Drying Behavior of Concrete: Influence of Drying Depth. *Materials and Structures*, 49(10):4029-4048.
- Shen, J., Dangla, P., Thiery, M., 2013. Reactive Transport Modeling of CO₂ through Cementitious Materials under CO₂ Geological Storage Conditions. *International Journal of Greenhouse Gas Control*, 18:75-87.
- Thiery, M., Dangla, P., Belin, P., Habert, G., Roussel, N., 2013. Carbonation Kinetics of a Bed of Recycled Concrete Aggregates: A Laboratory Study On Model Materials. *Cement and Concrete Research*, 46:50-65.
- Venhuis, M.A., Reardon, E.J., 2001. Vacuum Method for Carbonation of Cementitious Wasteforms. *Environmental Science & Technology*, 35(20):4120-4125.
- Xuan, D., Zhan, B., Poon, C.S., 2016. Assessment of Mechanical Properties of Concrete Incorporating Carbonated Recycled Concrete Aggregates. *Cement and Concrete Composites*, 65:67-74.
- Yang, C.C., Cho, S.W., 2003. Influence of Aggregate Content on the Migration Coefficient of Concrete Materials Using Electrochemical Method. *Materials Chemistry and Physics*, 80(3):752-757.
- Yu, M., Bao, H., Ye, J., Chi, Y., 2017. The Effect of Random Porosity Field on Supercritical Carbonation of Cement-Based Materials. *Construction and Building Materials*, 146:144-155.
- Zha, X., Yu, M., Ye, J., Feng, G., 2015. Numerical Modeling of Supercritical Carbonation Process in Cement-Based Materials. *Cement and Concrete Research*, 72:10-20.
- Zha, X., Wang, H., Xie, P., Wang, C., Dangla, P., Ye, J., 2016. Leaching Resistance of Hazardous Waste Cement Solidification after Accelerated Carbonation. *Cement and Concrete Composites*, 72:125-132.
- Zhan, B., Poon, C., Shi, C., 2013. CO₂ Curing for Improving the Properties of Concrete Blocks Containing Recycled Aggregates. *Cement and Concrete Composites*, 42:1-8.
- Zhang, J., Shi, C., Li, Y., Pan, X., Poon, C., Xie, Z., 2015. Influence of Carbonated Recycled Concrete Aggregate on Properties of Cement Mortar. *Construction and Building Materials*, 98:1-7.